Computer Simulation of Plaque formation and Development

Filipovic, D., Nenad; Meunier, Nicolas; Kojic, Milos; Isailovic, Velibor; Radovic, Milos; Milosevic, Zarko; Nikolic, Dalibor; Milasinovic, Danko; Exarchos, Themis; Parodi, Oberdan; and Fotiadis, Dimitris

Abstract—*Atherosclerosis develops from oxidized low-density lipoprotein molecules (LDL). When oxidized LDL evolves in plaque formations within an artery wall, a series of reactions occur to repair the damage to the artery wall caused by oxidized LDL. The body's immune system responds to the damage to the artery wall caused by oxidized LDL by sending specialized white blood cells-macrophages (Mphs) to absorb the oxidized-LDL forming specialized foam cells. Macrophages accumulate inside arterial intima. Also Smooth Muscle Cells (SMC) accumulate in the atherosclerotic arterial intima, where they proliferate and secrete extracellular matrix to form a fibrous cap.*

In this study, we simulate a process of atherosclerosis formation and development and compare it with literature data. The 3D blood flow is governed by the Navier-Stokes equations, together with the continuity equation. Mass transfer within the blood lumen and through the arterial wall is coupled with the blood flow and is modeled by the convection-diffusion equation. LDL transport in lumen of the vessel is described by Kedem-Katchalsky equations. The inflammatory process is solved using three additional reaction-diffusion partial differential equations.

The understanding and the prediction of the evolution of atherosclerotic plaques either into vulnerable plaques or into stable plaques are major tasks for the medical community.

Manuscript received March 1, 2011. This work was supported by European Commission (Project ARTREAT, ICT 224297).

N. D. Filipović, is with the Faculty of Mechanical Engineering, Kragujevac, Serbia (e-mail: fica@kg.ac.rs).

N. Meunier is with Paris Descartes University (Paris V),Paris, FRANCE, (e-mail: nicolas.meunier@math-info.univ-paris5.fr)

M. Kojic is with Bioengineering Research and Development Center, BioIRC, Kragujevac, Serbia, Harvard School of Public Health and Department of Nanomedicine and Biomedical Engineering, University of Texas Medical Center at Houston (e-mail: mkojic@hsph.harvard.edu)

V. Isailovic, M. Radovic, Z. Milosevic, D. Nikolic and D. Milasinovic are with the Research and Development Center for Bioengineering "BioIRC", Kragujevac, Serbia (phone: 381-34-301920; fax: 381-34-500089; e-mail: velibor@kg.ac.rs, mradovic@kg.ac.rs, zarko@kg.ac.rs, markovac85@kg.ac.rs, dmilashinovic@kg.ac.rs).

T. Exarchos and D. Fotiadis are with the Foundation of Research and Technology Hellas - Biomedical Research Institute, Ioannina, Greece and with the Unit of Medical Technology and Intelligent Information Systems, Dept of Material Science and Engineering, University of Ioannina, Ioannina, Greece. (email: exarchos@cc.uoi.gr, fotiadis@cc.uoi.gr)

O. Parodi is with the Instituto di Fisiologia Clinica, Consiglio Nazionale delle Ricerche, Pisa, Italy (email: oberpar@tin.it)

Index Terms — Atherosclerosis, Computer simulation, Plaque formation.

1. Introduction

ATHEROSCLEROSIS is a progressive disease characterized in particular by the accumulation of lipids and fibrous elements in artery walls. Over the past decade, scientists come to appreciate a prominent role for inflammation in atherosclerosis.

Atherosclerosis is characterized by dysfunction of endothelium, vasculitis and accumulation of lipid, cholesterol and cell elements inside blood vessel wall. This process develops in arterial walls. Atherosclerosis develops from oxidized low-density lipoprotein molecules (LDL). When oxidized LDL evolves in plaque formations within an artery wall, a series of reactions occur to repair the damage to the artery wall caused by oxidized LDL. The body's immune system responds to the damage to the artery wall caused by oxidized LDL by sending specialized white blood cells-macrophages (Mphs) to absorb the oxidized-LDL forming specialized foam cells. Macrophages accumulate inside arterial intima. Also Smooth Muscle Cells (SMC) accumulate in the atherosclerotic arterial intima, where they proliferate and secrete extracellular matrix to form a fibrous cap [1]. Unfortunately, macrophages are not able to process the oxidized-LDL, and ultimately grow and rupture, depositing a larger amount of oxidized cholesterol into the artery wall. The atherosclerosis process is shown in Fig. 1.

This chapter describes a completely new computer model for plaque formation and development. The first section is devoted to the LDL model of transport from the lumen to intima and detailed three-dimensional model for inflammatory and plaque progression process. The next section describes some of the benchmark examples for 2D, 2D axi-symmetric and 3D model of plaque formation and development. At the end a complex specific-patient 3D model is given. Finally the main conclusions of the work are addressed.

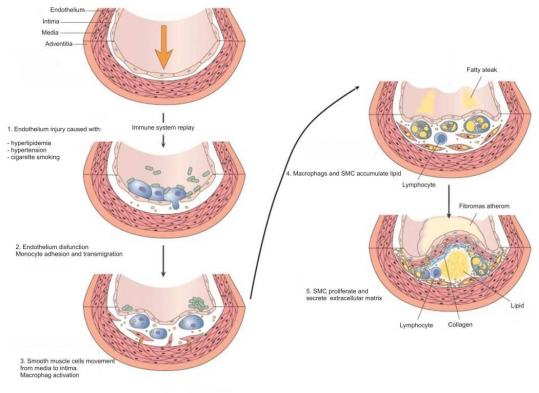

Figure 1: Atherosclerotic plaque development (adapted from [1])

2. METHODS

In this section a continuum based approach for plaque formation and development in three-dimension is presented. All algorithms are incorporated in program PAK-Athero from University of Kragujevac [2].

2.1 Governing equations for modeling of LDL transport through the arterial wall

The governing equations and numerical procedures are given. The blood flow is simulated by the three-dimensional Navier-Stokes equations, together with the continuity equation

$$-\mu\nabla^2 u_l + \rho(u_l\cdot\nabla)u_l + \nabla p_l = 0 \quad \text{Eq. (1)}$$

$$\nabla u_l = 0 \quad \text{Eq. (2)}$$

where $\boldsymbol{u_l}$ is blood velocity in the lumen, $p_l$is the pressure, μ is the dynamic viscosity of the blood, and ρ is the density of the blood.

Mass transfer in the blood lumen is coupled with the blood flow and modelled by the convection-diffusion equation as follows

$$\nabla\cdot\left(-D_l\nabla c_l + c_l u_l\right) = 0 \quad \text{Eq. (3)}$$

in the fluid domain, where c_l is the solute concentration in the blood lumen, and D_l is the solute diffusivity in the lumen.

Mass transfer in the arterial wall is coupled with the transmural flow and modelled by the convection-diffusion-reaction equation as follows

$$\nabla\cdot\left(-D_w\nabla c_w + k c_w u_w\right) = r_w c_w \quad \text{Eq. (4)}$$

in the wall domain, where c_w is the solute concentration in the arterial wall, D_w is the solute diffusivity in the arterial wall, K is the solute lag coefficient, and r_w is the consumption rate constant.

LDL transport in lumen of the vessel is coupled with Kedem-Katchalsky equations:

$$J_v = L_p\left(\Delta p - \sigma_d\Delta\pi\right) \quad \text{Eq. (5)}$$

$$J_s = P\Delta c + \left(1-\sigma_f\right)J_v\bar{c} \quad \text{Eq. (6)}$$

where L_p is the hydraulic conductivity of the endothelium, Δc is the solute concentration difference across the endothelium, Δp is the pressure drop across the endothelium, $\Delta\pi$ is the oncotic pressure difference across the endothelium, σ_d is the osmotic reflection coefficient, σ_f is the solvent reflection coefficient, P is the solute endothelial permeability, and $\bar{c}$ is the mean endothelial concentration.

The basic relations for mass transport in the artery. The metabolism of the artery wall is critically dependent upon its nutrient supply governed by transport processes within the blood. A two different mass transport processes in large arteries are addressed. One of them is the oxygen transport and the other is LDL transport. Blood flow through the arteries is usually described as motion of a fluid-type continuum, with the wall surfaces treated as impermeable (hard) boundaries. However, transport of gases (e.g. O_2, CO_2) or macromolecules (albumin, globumin, LDL) represents a convection-diffusion physical process with permeable boundaries through which the diffusion occurs. In the analysis presented further, the assumption is that the concentration of the transported matter does not affect the blood flow (i.e. a diluted mixture is considered). The mass transport process is governed by convection-diffusion equation,

$$\frac{\partial c}{\partial t} + v_x\frac{\partial c}{\partial x} + v_y\frac{\partial c}{\partial y} + v_z\frac{\partial c}{\partial z} = D\left(\frac{\partial^2 c}{\partial x^2} + \frac{\partial^2 c}{\partial y^2} + \frac{\partial^2 c}{\partial z^2}\right) \quad \text{Eq. (7)}$$

where c denotes the macromolecule or gas concentration; v_x, v_y and v_z are the blood velocity components in the coordinate system x,y,z; and D is the diffusion coefficient, assumed constant, of the transported material.

Boundary conditions for transport of the LDL. A macromolecule directly responsible for the process of atherosclerosis is LDL which is well known as atherogenic molecule. It is also known that LDL can go through the endothelium at least by three different mechanisms, namely, receptor-mediated endocytosis, pinocytotic vesicular transport, and phagocytosis [3]. The permeability coefficient of an intact arterial wall to LDL has been reported to be of the order of 10^{-8} [*cm*/*s*] [4]. The conversion of the mass among the LDL passing through a semipermeable wall, moving toward the vessel wall by a filtration flow and diffusing back to the mainstream at the vessel wall, is described by the relation

$$c_w v_w - D\frac{\partial c}{\partial n} = K c_w \quad \text{Eq. (8)}$$

where c_w is the surface concentration of LDL, v_w is the filtration velocity of LDL transport through the wall, n is coordinate normal to the wall, D is the diffusivity of LDL, and K is the overall mass transfer coefficient of LDL at the vessel wall. A uniform constant concentration C_0 of LDL is applied at the artery tree inlet as classical inlet boundary condition for eq. (7).

2.2 Finite Element Modeling of Diffusion-Transport Equations

In the case of blood flow with mass transport we have domination of the convection terms due to the low diffusion coefficient [5]. Then it is

necessary to employ special stabilizing techniques in order to obtain a stable numerical solution. The streamline upwind/Petrov-Galerkin stabilizing technique (SUPG) [6] within a standard numerical integration scheme is implemented. The incremental-iterative form of finite element equations of balance are obtained by including the diffusion equations and transforming them into incremental form. The final equations are

$$\begin{bmatrix} \frac{1}{\Delta t}\mathbf{M}_v + {}^{n+1}\mathbf{K}_{vv}^{(i-1)} + {}^{n+1}\mathbf{K}_{pv}^{(i-1)} + {}^{n+1}\mathbf{J}_{vv}^{(i-1)} & {}^{n+1}\mathbf{K}_{vp}^{(i-1)} & \mathbf{0} \\ \mathbf{K}_{vp}^{\mathrm{T}} & \mathbf{0} & \mathbf{0} \\ {}^{n+1}\mathbf{K}_{cv}^{(i-1)} & \mathbf{0} & \frac{1}{\Delta t}\mathbf{M}_c + {}^{n+1}\mathbf{K}_{cc}^{(i-1)} + {}^{n+1}\mathbf{J}_{cc}^{(i-1)} \end{bmatrix} \times \begin{Bmatrix} \Delta\mathbf{V}^{(i)} \\ \Delta\mathbf{P}^{(i)} \\ \Delta\mathbf{C}^{(i)} \end{Bmatrix} = \begin{Bmatrix} {}^{n+1}\mathbf{F}_v^{(i-1)} \\ {}^{n+1}\mathbf{F}_p^{(i-1)} \\ {}^{n+1}\mathbf{F}_c^{(i-1)} \end{Bmatrix} \quad \text{Eq. (9)}$$

where the matrices are

$$(\mathbf{M}_v)_{jiKJ} = \int_V \rho N_K N_J dV, \qquad (\mathbf{M}_c)_{jiKJ} = \int_V N_K N_J dV \quad \text{Eq. (10)}$$

$$\left({}^{n+1}\mathbf{K}_{cc}^{(i-1)}\right)_{jiKJ} = \int_V D N_{K,j} N_{J,j} dV \qquad \left({}^{n+1}\mathbf{K}_{pv}^{(i-1)}\right)_{jiKJ} = \int_V \mu N_{K,j} N_{J,j} dV$$

$$\left({}^{n+1}\mathbf{K}_{cv}^{(i-1)}\right)_{jiKJ} = \int_V N_K \, {}^{n+1}c_{,j}^{(i-1)} N_J dV \qquad \left({}^{n+1}\mathbf{K}_{vv}^{(i-1)}\right)_{jiKJ} = \int_V \rho N_K \, {}^{n+1}v_j^{(i-1)} N_{J,j} dV$$

$$\left({}^{n+1}\mathbf{J}_{cc}^{(i-1)}\right)_{jiKJ} = \int_V \rho N_K \, {}^{n+1}v_j^{(i-1)} N_{J,j} dV \qquad \left({}^{n+1}\mathbf{K}_{vp}^{(i-1)}\right)_{jiKJ} = \int_V \rho N_{K,j} \hat{N}_J dV$$

$$\left({}^{n+1}\mathbf{J}_{vv}^{(i-1)}\right)_{jikJ} = \int_V \rho N_K \, {}^{n+1}v_{j,k} N_J dV$$

and the vectors are

$${}^{n+1}\mathbf{F}_c^{(i-1)} = {}^{n+1}\mathbf{F}_q + {}^{n+1}\mathbf{F}_{sc}^{(i-1)} - \frac{1}{\Delta t}\mathbf{M}_c\left\{{}^{n+1}\mathbf{C}^{(i-1)} - {}^{n}\mathbf{C}\right\} - {}^{n+1}\mathbf{K}_{cv}^{(i-1)}\left\{{}^{n+1}\mathbf{V}^{(i-1)}\right\} - {}^{n+1}\mathbf{K}_{cc}^{(i-1)}\left\{{}^{n+1}\mathbf{C}^{(i-1)}\right\} \quad \text{Eq. (11)}$$

$$\left({}^{n+1}\mathbf{F}_q\right)_K = \int_V N_K q^B dV \qquad {}^{n+1}\mathbf{F}_{sc}^{(i-1)} = \int_S D N_K \nabla \, {}^{n+1}\mathbf{c}^{(i-1)} \cdot \mathbf{n} dS$$

Note that $\hat{N}_J$ are the interpolation functions for pressure (which are taken to be for one order of magnitude lower then interpolation functions N_I for velocities). The matrices $\mathbf{M}_{cc}$ and $\mathbf{K}_{cc}$ are the 'mass' and convection matrices; $\mathbf{K}_{cv}$ and $\mathbf{J}_{cc}$ correspond to the convective terms of equation (7); and $\mathbf{F}_c$ is the force vector which follows from the convection-diffusion equation in (7) and linearization of the governing equations.

2.3 Modeling of Plaque Formation and Development

The inflammatory process was solved using three additional reaction-diffusion partial differential equations [7, 8]:

$$\begin{aligned} \partial_t Ox &= d_2 \Delta Ox - k_1 Ox \cdot M \\ \partial_t M + div(v_w M) &= d_1 \Delta M - k_1 Ox \cdot M + S/(1-S) \\ \partial_t S &= d_3 \Delta S - \lambda S + k_1 Ox \cdot M + \gamma(Ox - Ox^{thr}) \end{aligned} \quad \text{Eq. (12)}$$

where Ox is the oxidized LDL or cw - the solute concentration in the wall from eq. (7);M and S are concentrations in the intima of macrophages and cytokines, respectively; d1,d2,d3 are the corresponding diffusion coefficients; λ and γ degradation and LDL oxidized detection coefficients; and vwis the inflammatory velocity of plaque growth, which satisfies Darcy's law and continuity equation [5, 9, 10, 11]:

$$v_w - \nabla \cdot (p_w) = 0 \quad \text{Eq. (13)}$$

$$\nabla v_w = 0 \quad \text{Eq. (14)}$$

in the wall domain. Here, $p_w$is the pressure in the arterial wall.

3. RESULTS

3.1 2D Model of Plaque Formation and Development

For the first example of a two-dimensional model of the mild stenosis, a fully developed parabolic steady velocity profile was assumed at the lumen inlet boundary

$$u(r) = 2U_0\left(1 - \left(\frac{2r}{D}\right)^2\right) \quad \text{Eq. (15)}$$

where $u(r)$ is the velocity in the axial direction at radial position r; D is the inlet diameter; and U_0 is the mean inlet velocity. At the lumen side of the endothelial boundary, a lumen-to-wall transmural velocity in the normal direction was specified:

$$t_l^T \cdot u_l = 0 \quad \text{Eq. (16)}$$

$$u_l n_l = J_v$$

where $\boldsymbol{t_l^T}$ and $\boldsymbol{n_l}$ are the tangential and normal unit vectors of fluid subdomain, respectively.
Oxidized LDL distribution for a mild stenosis is shown in Fig. 2.

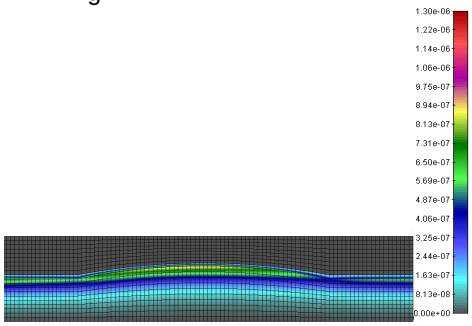

Figure 2: Oxidized LDL distribution for a mild stenosis (30% constriction by area)

3.2 2D axi-symmetric model of plaque formation and development

The plaque formation and development is modeled through an initial straight artery in 2D axi-symmetric model with mild constriction of 30%. The inlet artery diameter d_0=0.4 [*cm*]. Blood was modeled as a Newtonian fluid with density $\rho = 1.0$ [g/cm^3] and viscosity $\mu = 0.0334$ [*P*]. The steady state conditions for fluid flow and mass transport are assumed. The entering blood velocity is defined by the Reynolds number Re (calculated using the mean blood velocity and the artery diameter).

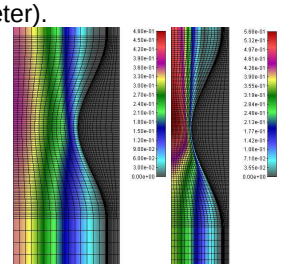

Figure 3: a) Velocity distribution for an initial mild stenosis 30% constriction by area b) Velocity distribution at the end of stenosis process after 10^7 sec [units m/s]

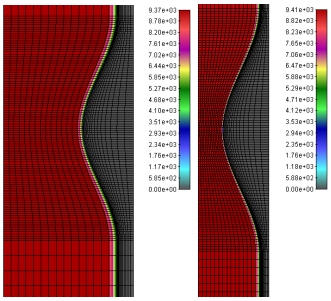

Figure 4: a) Pressure distribution for an initial mild stenosis 30% constriction by area b) Pressure distribution at the end of stenosis process after 10^7 sec[units Pa]

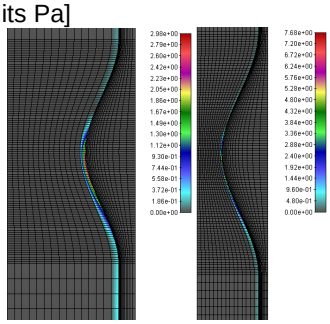

Figure 5: a) Shear stress distribution for an initial mild stenosis 30% constriction by area b) Shear stress distribution at the end of stenosis process after 10^7 sec[unitsdyn/cm^2]

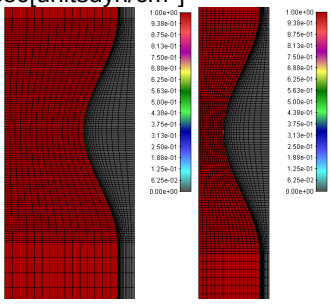

Figure 6: a) Lumen LDL distribution for an initial mild stenosis 30% constriction by area b) Lumen LDL distribution at the end of stenosis process after 10^7 sec[units mg/mL]

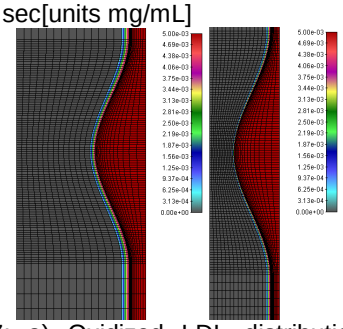

Figure 7: a) Oxidized LDL distribution in the intima for an initial mild stenosis 30% constriction by area b) Oxidized LDL distribution in the intima at the end of stenosis process after 10^7sec[units mg/mL]

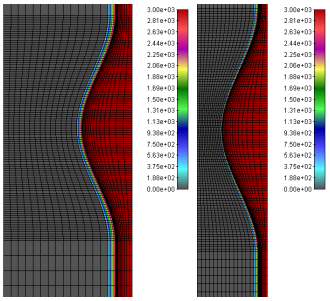

Figure 8: a) Intima wall pressure distribution for an initial mild stenosis 30% constriction by area b) Intima wall pressure distribution at the end of stenosis process after 10^7sec[units Pa]

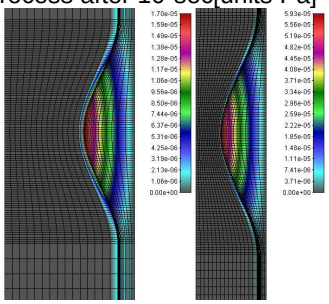

Figure 9: a) Macrophages distribution in the intima for an initial mild stenosis 30% constriction by area b) Macrophages distribution in the intima at the end of stenosis process after 10^7 sec[units mg/mL]

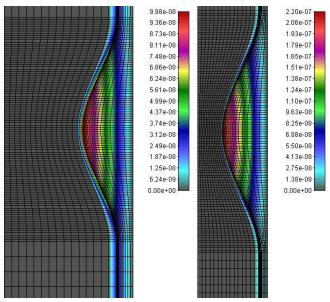

Figure 10: a) Cytokines distribution in the intima for an initial mild stenosis 30% constriction by area b) Cytokines distribution in the intima at the end of stenosis process after 10^7 sec[units mg/mL]

3.3 3D Model of Plaque Formation and Development

In order to make benchmark example for three-dimensional simulation we tested simple middle stenosis with initial 30% constriction for time period of t=10^7 sec (approximately 7 years) and compare results with 2D axi-symmetric model. The results for velocity distribution for initial and end stage of simulations are presented in Fig. 11a and Fig. 11b. The pressure and shear stress distributions for start and end time are given in Fig. 12 and Fig. 13. Concentration distribution of LDL inside the lumen domain and oxidized LDL inside the intima are presented in Fig. 14 and Fig. 15.The transmural wall pressure is presented in Fig. 16. Macrophages and cytokines distributions are shown in Fig. 17 and Fig. 18.The diagram of three-dimensional plaque volume growing during time is given in Fig. 19. It can be seen that time period for developing of

stenosis corresponds to data available in the literature [12].

a)

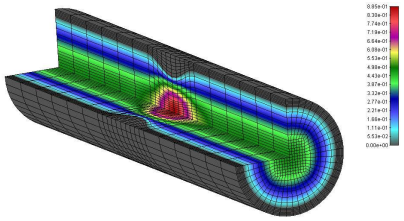

b)

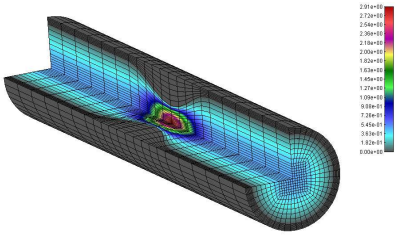

Figure 11: a) Velocity distribution for an initial mild stenosis 30% constriction by area b) Velocity distribution at the end of stenosis process after 10^7 sec[unitsm/s]

a)

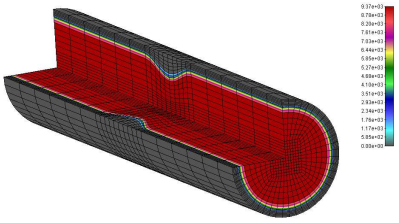

b)

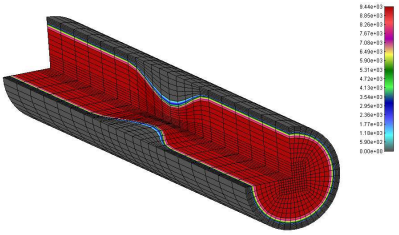

Figure 12: a) Pressure distribution for an initial mild stenosis 30% constriction by area b) Pressure distribution at the end of stenosis process after 10^7 sec[units Pa]

a)

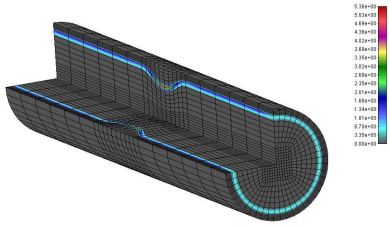

b)

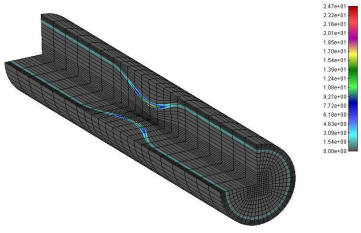

Fig. 13. a) Shear stress distribution for an initial mild stenosis 30% constriction by area b) Shear stress distribution at the end of stenosis process after 10^7 sec[unitsdyn/cm^2]

a)

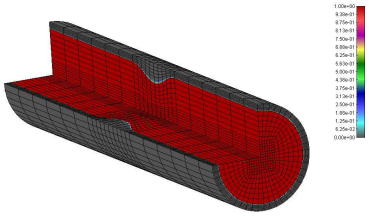

b)

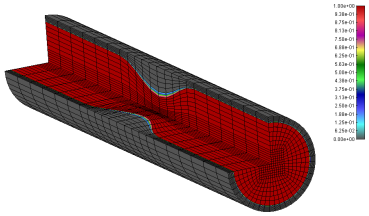

Figure 14: a) Lumen LDL distribution for an initial mild stenosis 30% constriction by area b) Lumen LDL distribution at the end of stenosis process after 10^7 sec[units mg/mL]

a)

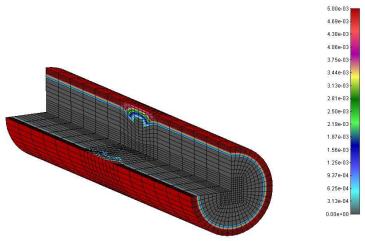

b)

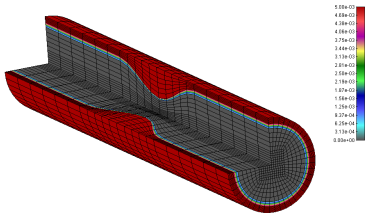

Figure 15: a) Oxidized LDL distribution in the intima for an initial mild stenosis 30% constriction by area b) Oxidized LDL distribution in the intima at the end of stenosis process after 10^7 sec[units mg/mL]

a)

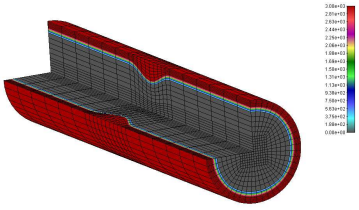

b)

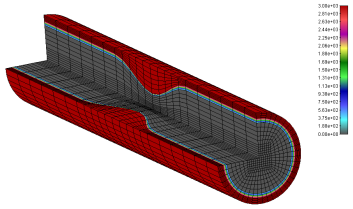

Figure 16: a) Intima wall pressure distribution for an initial mild stenosis 30% constriction by area b)

Intima wall pressure distribution at the end of stenosis process after 10^7 sec[units Pa]

a)

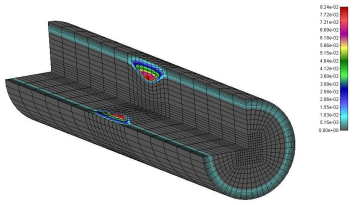

b)

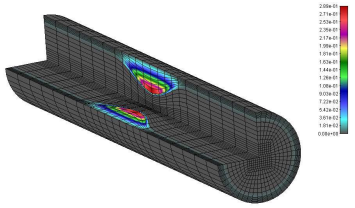

Figure 17: a) Macrophages distribution in the intima for an initial mild stenosis 30% constriction by area b) Macrophages distribution in the intima at the end of stenosis process after 10^7 sec[units mg/mL]

a)

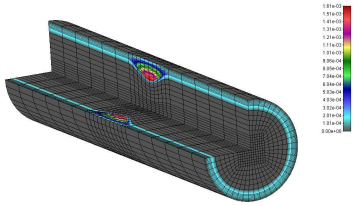

b)

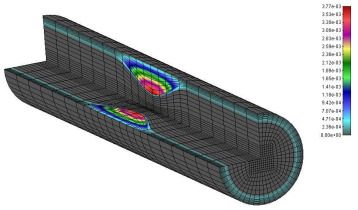

Figure 18: a) Cytokines distribution in the intima for an initial mild stenosis 30% constriction by area b) Cytokines distribution in the intima at the end of stenosis process after 10^7 sec[units mg/mL]

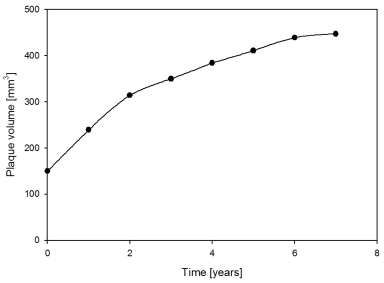

Figure 19: Plaque progression during time (computer simulation)

From above figures it can be observed that during time plaque is progressing and all the variables as velocity distribution, shear stress, macrophages, cytokines are increasing. Also from Fig. 19 it can be seen that plaque progression in volume during time corresponds to clinical findings [13].

The last example is a model of the patient specific Left Anterior Descending(LAD)coronary artery for steady flow conditions. Computed concentration of LDL indicates that there is a newly formed matter in the intima, especially in the flow separation region in the LAD artery (Fig. 20).

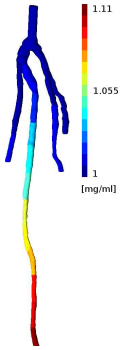

Figure 20: LDL concentration distribution in the left anterior descending coronary artery

4. Discussion and Conclusions

Full three-dimensional model was created for plaque formation and development, coupled with blood flow and LDL concentration in blood. The models for plaque initiation and plaque progression are developed. These two models are based on partial differential equations with space and times variables and they describe the biomolecular process that takes place in the intima during the initiation and the progression of the plaque.The model for plaque formation and plaque progression despite some difficulties concerning the different time scales that are involved and the different blood velocities in the lumen and in the intima, its numerical treatment is developed by using decomposition techniques together with finite elements methods and by splitting the numerical scheme into three independent parts: blood flow and LDL transfer, inflammatory process and atheromatous plaque evolution.

Determination of plaque location and progression in time for a specific patient shows a potential benefit for future prediction of this vascular decease using computer simulation. The understanding and the prediction of the evolution of atherosclerotic plaques either into vulnerable plaques or into stable plaques are major tasks for the medical community.

Acknowledgment

This work is part funded by European Commission (Project ARTREAT, ICT 224297).

References

[1] Loscalzo, J., Schafer, A. I., “Thrombosis and Hemorrhage,” Third edition, Lippincott Williams & Wilkins, 978-0781730662, Philadelphia, 2003.

[2] Filipovic, N., Meunier, N., Kojic, M., “PAK-Athero, Specialized three-dimensional PDE software for simulation of plaque formation and development inside the arteries,” University of Kragujevac, 34000 Kragujevac, Serbia, 2010.

[3] Goldstein, J., Anderson, R., Brown, M., “Coated pits, coated vesicles, and receptor-mediated endocytosis,” Nature, 1979, 279, pp. 679-684.

[4] Bratzler, R. L., Chisolm, G.M., Colton, C. K., Smith, K. A., Lees, R.S., “The distribution of labeled low-density lipoproteins across the rabbit thoracic aorta in vivo,” Atherosclerosis, 1977, 28(3), pp. 289–307.

[5] Kojic, M., Filipovic, N., Stojanovic, B., Kojic, N., “Computer Modeling in Bioengineering – Theoretical Background, Examples and Software,” John Wiley and Sons, 978-0-470-06035-3, England. 2008.

[6] Brooks, A. N., Hughes, T. J. R., “Streamline upwind/Petrov-Galerkin formulations for convection dominated flows with particular emphasis on the incompressible Navier-Stokes equations,” *Comput. Meths. Appl. Mech. Engrg.*, 1982, 32(1-3), pp. 199-259.

[7] Calvez, V., Ebde, A., Meunier, N., Raoult, A., “Mathematical modelling of the atherosclerotic plaque formation,” Proceedings of ESAIM, 2008, 28, pp. 1-12.

[8] Boynard, M., Calvez, V., Hamraoui, A., Meunier. N., Raoult, A., “Mathematical modelling of earliest stage of atherosclerosis,” *Proceedings of* COMPDYN 2009 - SEECCM 2009, Rhodes, 2009.

[9] Filipovic, N., Kojic, M., “Computer simulations of blood flow with mass transport through the carotid artery bifurcation,” Theoret. Appl. Mech. (Serbian), 2004, 31(1), pp. 1-33.

[10] Filipovic, N., Mijailovic, S., Tsuda, A., Kojic, M., “An Implicit Algorithm Within The Arbitrary Lagrangian-Eulerian Formulation for Solving Incompressible Fluid Flow With Large Boundary Motions,” *Comp. Meth. Appl. Mech. Eng.*, 2006a, 195(44-47), pp. 6347-6361.

[11] Filipovic, N., Kojic, M., Ivanovic, M., Stojanovic, B., Otasevic, L., Rankovic, V., “MedCFD, Specialized CFD software for simulation of blood flow through arteries,” University of Kragujevac, 34000 Kragujevac, Serbia, 2006b.

[12] Goh, V. K., Lau, C. P., Mohlenkamp, S., Rumberger, J. A., Achenbach A., Budoff, M. J., “Outcome of coronary plaque burden: a 10-year follow-up of aggressive medical management,” Cardiovascular Ultrasound, 2010, 8:5.

[13] Verstraete, M., Fuster, V., Topol, E. J., “Cardiovascular Thrombosis: Thrombocardiology and Thromboneurology,” Second Edition, Lippincot-Raven Publishers, 978-0397587728, Philadelphia, 1998.

[14] Caro, C. G., Fitz-Gerald, J. M., Schroter, R. C., “Atheroma and Arterial Wall Shear. Observation, Correlation and Proposal of a Shear Dependent Mass Transfer Mechanism for Atherogenesis,” Proc. R. Soc. London, 1971, 177(46), pp. 109–159.